Hydraulic conductivity of the matric porosity of an unsaturated vertisol : a field and laboratory comparison

Stephane Ruy, Yves-Marie Cabidoche

Hydraulic conductivity of the matric porosity of an unsaturated Vertisol: a field and laboratory comparison.

S. RUY[*] & Y.M. CABIDOCHE

Unité Agropédoclimatique de la Zone Caraïbe, INRA, BP 515, 97 165 Pointe-à-Pitre Cedex, Guadeloupe, French West Indies.

Head title: *Matric conductivity of a Vertisol*

Summary

In many swelling clay soils several types of porosity can be defined: matric, structural and crack porosities. Measuring the hydraulic conductivity associated with the matric porosity is of major interest because soil movements are governed by matric water flows. Our purpose was to determine the matric conductivity of a vertisol from Guadeloupe (French West Indies) under laboratory and field conditions. We used an Eulerian flow description to measure the conductivity of natural vertisol clods in the laboratory with a drying method. In order to take into account soil movements in every direction, we introduced a tensorial analysis of soil deformations and hydraulic conductivity. The instantaneous profile method was used in the field under wetting conditions. Using soil layer thickness transducers we described water flows in a material coordinate system that can deal with volumetric soil deformations. For wet soil the ratio between the hydraulic conductivity measured in the field and that measured at the laboratory ranged around 10. However, because the spatial variation of the water content was large, no final conclusion could be drawn to explain this discrepancy. We showed that the gradient of the overburden potential was smaller than that of the matric potential in the field

[*] Correspondence: S. Ruy, Unité de Science du Sol, INRA, Domaine St Paul, Site Agroparc, 84 914 Avignon Cedex 9, France. E-mail: ruy@avignon.inra.fr

experiment.

Mesure de la conductivité hydraulique matricielle d'un vertisol: comparaison laboratoire - terrain.

Résumé

Dans de nombreux sols argileux gonflants, tels que les vertisols de Guadeloupe, coexistent des compartiments de porosité (matricielle, structurale, fissurale) au sein desquels les vitesses de transfert d'eau diffèrent fortement et entre lesquels les échanges sont fortement limités. La connaissance de la courbe de conductivité hydraulique de la matrice du sol est de première importance car elle va déterminer la vitesse d'ouverture et de fermeture des fissures. Nous utilisons une approche eulérienne au laboratoire pour obtenir la courbe de conductivité hydraulique matricielle au sens de Darcy sur des échantillons de vertisol non remaniés, en utilisant la méthode des profils instantanés en dessiccation. L'écriture de la conductivité hydraulique apparente sous forme tensorielle non diagonale permet de prendre en compte un retrait tridimensionnel de l'échantillon. Nous mesurons ensuite la courbe de conductivité matricielle au champ par un suivi en réhumectation. L'utilisation de transducteurs d'épaisseurs de couches nous conduit à utiliser un repère matériel. Les équations développées dans ce repère permettent de prendre en considération les mouvements du sol dans les trois directions de l'espace. Pour de fortes teneurs en eau, le rapport entre la conductivité hydraulique mesurée *in situ* et celle mesurée au laboratoire est de l'ordre de 10. Nos résultats obtenus au champ, entachés d'une forte variabilité spatiale de la teneur en eau, ne permettent pas de conclure de façon définitive sur la cause de cette différence. Nous avons montré que l'influence du potentiel pédostatique au champ était nulle sur les propriétés du sol mesurées, et mineure sur le calcul de la conductivité, à cause de faibles gradients en comparaison des gradients du potentiel matriciel.

Introduction

In swelling clay soils, and especially in vertisols, successive cycles of wetting and drying induce volumetric deformation and changes of porosity. These movements can be followed by subsidence or collapse of the soil's surface and crack formation. On the basis of hydraulic criteria, three kinds of porosities can be defined. These are as follows.

1 *A network of vertical cracks*, which delimits the continuous peds or prisms containing a system of fine pores and a system of larger structural pores (Stirk, 1954). This network is more or less regular, and water flows inside these cracks rapidly.

2 *The Matric porosity*. A system of fine pores, hereafter called *Matric porosity*, is formed by the arrangement of clay particles. It remains saturated during structural and normal shrinkage (as defined by Stirk, 1954) and thus contains the water responsible for soil movement.

3 *The Structural porosity* is formed by macropores and mesopores (McIntyre & Sleeman, 1982). It is formed by the soil mesofauna, microbial activity and root paths. Structural water does not induce any deformation of the soil (Ritchie *et al.*, 1972b).

Because cracks are present, it is difficult to measure the hydraulic conductivity of the whole unsaturated soil and to determine its significance. The representative elementary volume should represent several cubic metres, and naturally occurring water flow inside these cracks cannot be described by Darcy's law. When dealing with the conductivity of the prisms other difficulties arise. As emphasized by Cabidoche & Ozier-Lafontaine (1995), structural and matric flows are almost independent. The structural porosity can be filled with water at any matric water content, and water moves from structural to matric porosity very slowly. Thus, water potentials can be horizontally heterogeneous inside the prisms. It is therefore necessary to separate matric and structural water flows.

Few investigators have measured the conductivity of an unsaturated vertisol in the field. Tension infiltrometers were successfully used for swelling soils (Jarvis *et al.*, 1987).

Nevertheless, the range of suctions made it possible to obtain the conductivity of the structural porosity only (Jarvis & Messing, 1995). Douglas *et al.* (1980) used the internal drainage method in a material coordinate system, assuming that soil deformation was only vertical.

Ritchie *et al.* (1972b) determined the hydraulic conductivity of undisturbed unsaturated vertisol cores in the laboratory. They used the pressure plate outflow method to measure the water diffusivity in the soil without taking into account soil movement. This method was approximate. Many other authors worked on clay paste using a material coordinate system which assumes that soil deformation occurs in one direction only (*e.g.* Smiles & Harvey, 1973; Douglas & McKyes, 1978). Garnier (1996) used an inverse modelling method to determine the hydraulic conductivity of a remodelled vertisol: water fluxes were described in a Lagrangian coordinate system (Raats & Klute, 1968, 1969) and the soil deformed in every direction. Nakano *et al.* (1986) and Angulo *et al.* (1990a) used a fixed (Eulerian) coordinate system to describe water and solid flows. By relating solid and water potentials, they could measure the Darcian hydraulic conductivity (Nakano *et al.*, 1986; Angulo *et al.*, 1990b), but deformation was only one-dimensional.

When determining the hydraulic conductivity of undisturbed unsaturated swelling soils in the laboratory, one must do so as the soil dries. Indeed, when the soil rewets and swells, it can be laterally limited by the rigid sides of the core sampler, thus inducing a bias in the determination of the soil's characteristics (Bronswijk, 1990). In this respect, the method used by Kim *et al.* (1992a) is questionable. They used the falling head method on a saturated clay paste with different moisture ratios, but the core was not allowed to swell. Kim *et al.* (1992b) recorded tensiometer pressure profiles and elevation changes of a remodelled clay soil as it dried. The distances between tensiometers were corrected based on measurements of height, as were the cross sections of the core, because of a differential shrinkage between the surface and the bottom of the core.

In our study we measured the matric hydraulic conductivity of an undisturbed

unsaturated vertisol from Guadeloupe in the laboratory and in the field. In the laboratory we determined this conductivity under drying conditions by using an Eulerian coordinate system taking into account soil movements in every direction. In such a coordinate system, water and solid flows must be described. We defined the initial conditions, so that the structural porosity was filled with air, and water flowed only in the matric porosity. In the field, matric flow was described in a material or Lagrangian coordinate system using transducers that measured thickness variations of soil layers as the soil rewetted. In both theories water and solid flows are related to a unit cross-section of prism and not of soil. This is justified in two ways.

1 From a continuum point of view, the continuity of local variables (water and solid contents, water potential) is interrupted by the crack walls.

2 The soil behaviour (the appearance and disappearance of cracks) depends only on the matric flow, which is governed by the matric potential and matric hydraulic conductivity.

As the two methods are independent, we first present the theory and methods used in the laboratory and then those for the field.

Theory, materials and methods

Soil

The soil is a chromic vertisol from Guadeloupe (French West Indies) at la Simonière in St François (16°7'57" N, 61°19'03" W, 34 m elevation). Based on the results of Cabidoche & Ozier-Lafontaine (1995), we supposed that there was no water exchange from structural to matric porosities.

Laboratory measurements: theory

The soil is considered as a three-phase system: water, air and solid particles, each phase being in motion. The air flow is neglected. As water and solid are both in motion, we can describe water and solid flows in a fixed Eulerian coordinate system (subscript /o) or in a moving coordinate system linked to the solid flow (subscript /s). Hereafter, subscript w refers to water

and subscript s to solid. The following hypotheses are supposed to be satisfied:

1 - the matric porosity is homogeneous and isotropic,

2 - solid particles are incompressible and chemically inert,

3 - water is incompressible and pure,

4 - water flow is isothermal and hydrodynamically stable,

5 - the flow of water vapor and the phase transition of water are not significant,

6 - a unique representative elementary volume can be defined for all the variables and parameters,

7 - there are no sinks and sources,

8 - Darcy's law is valid for water flow,

9 - the solid flow is described by the following phenomenological transfer equation:

$$\mathbf{q}_{s/o} = -\mathbf{K}_{s/o} \cdot \vec{\nabla} \psi_s, \tag{1}$$

where $\mathbf{q}_{s/o}$ is the solid flow, $\mathbf{K}_{s/o}$ is the tensorial apparent solid conductivity, ψ_s is the solid potential which depends on the solid content only, and $\vec{\nabla}$ is the vector differential operator. Hypotheses 1 to 8 originate from Vauclin (1988), and hypothesis 9 originates from Nakano *et al.* (1986) and Angulo *et al.* (1990a).

From hypotheses 2 to 6 it can be deduced that the total water potential ϕ is the sum of the matric potential ψ_m (the opposite of the suction), the gravimetric potential $-z$ (assuming the vertical axis to be positive downward) and the overburden potential Ω (Philip, 1969). Hereafter, gravimetric and overburden potential will be neglected because of their small values (a few centimetres) compared with that of the matric potential (several hundreds of centimetres). If we suppose that the water content is uniform in the horizontal plane then both solid and water potentials are uniform in the plane. Thus Darcy's law in both a fixed and moving coordinate system and Equation (1) for solid particles can be written as:

$$\begin{cases} \mathbf{q}_{w/o} = -\mathbf{K}_{w/o} \cdot \left(\dfrac{\partial \psi_m}{\partial z} \cdot \mathbf{e}_z \right) & \text{(2a)} \\[2em] \mathbf{q}_{w/s} = -\mathbf{K}_{w/s} \cdot \left(\dfrac{\partial \psi_m}{\partial z} \cdot \mathbf{e}_z \right) & \text{(2b)} \\[2em] \mathbf{q}_{s/o} = -\mathbf{K}_{s/o} \cdot \left(\dfrac{\partial \psi_s}{\partial z} \cdot \mathbf{e}_z \right) , & \text{(2c)} \end{cases}$$

where $\mathbf{q}$ is the flux and $\mathbf{e}_z$ is the unit vector of the vertical axis. Symmetrical tensorial conductivities are written:

$$\mathbf{K} = \begin{bmatrix} K^{xx} & K^{xy} & K^{xz} \\ K^{xy} & K^{yy} & K^{yz} \\ K^{xz} & K^{yz} & K^{zz} \end{bmatrix} . \tag{3}$$

If we suppose that the soil is not stratified (hypothesis 1), then the hydraulic conductivity $\mathbf{K}_{w/s}$ is isotropic and reduces to a scalar $K_{w/s}$. On the contrary, it is worth pointing out that the soil behaves as if it was stratified in the Eulerian coordinate system: the potential gradients are only vertical, but the movements of water and solid occur in every direction (for instance, see the cracks opening following a vertical evaporation). This leads us to consider the apparent hydraulic conductivity $\mathbf{K}_{w/o}$ and the apparent solid conductivity $\mathbf{K}_{s/o}$ as a tensorial property.

From hypothesis 1 it can be deduced that the water flow with respect to the fixed coordinate system is related to the water flow relative to the soil particles and to the flow of soil particles by the following equation:

$$\mathbf{q}_{w/o} = \mathbf{q}_{w/s} + \frac{\theta}{\sigma} \cdot \mathbf{q}_{s/o}, \tag{4}$$

where θ and σ are the water and solid contents. According to Nakano *et al.* (1986) and Angulo *et al.* (1990a), the relation between solid and water potentials is assumed to be:

$$\frac{\partial \psi_s}{\partial z} = -\nu \cdot \frac{\partial \psi_w}{\partial z}, \; \nu \in [0,1]. \tag{5}$$

The negative sign indicates that $\dfrac{\partial \psi_s}{\partial z}$ and $\dfrac{\partial \psi_w}{\partial z}$ act in opposite directions. In a saturated porous medium ψ_s and ψ_w are analogous to the effective mechanical stress and to the pore

water pressure, respectively, and v is equal to 1 (Angulo *et al.*, 1990a). By combining Equations (2), (4) and (5) we have in the vertical direction:

$$K_{w/o}^{zz} = K_{w/s} - v \cdot \frac{\theta}{\sigma} \cdot K_{s/o}^{zz}. \tag{6}$$

The aim is now to eliminate v.

Instead of using the hydraulic conductivities in Equation (2), we can use the diffusivity tensors that are related to conductivities by the usual relation:

$$\begin{cases} \mathbf{D}_{w/o} = \mathbf{K}_{w/o} \cdot \dfrac{\mathrm{d}\,\psi_w}{\mathrm{d}\,\theta} \\[3mm] \mathbf{D}_{s/o} = \mathbf{K}_{s/o} \cdot \dfrac{\mathrm{d}\,\psi_s}{\mathrm{d}\,\sigma} \end{cases}. \tag{7}$$

Thus, the combination of Equations (2), (7) and (5) implies

$$\frac{D_{s/o}^{zz}}{D_{w/o}^{zz}} = \frac{K_{s/o}^{zz}}{K_{w/o}^{zz}} \cdot \frac{\mathrm{d}\,\psi_s}{\mathrm{d}\,\psi_w} \cdot \frac{\mathrm{d}\,\theta}{\mathrm{d}\,\sigma}$$

$$\Updownarrow$$

$$\frac{D_{s/o}^{zz}}{D_{w/o}^{zz}} = -v \cdot \frac{K_{s/o}^{zz}}{K_{w/o}^{zz}} \cdot \frac{\mathrm{d}\,\theta}{\mathrm{d}\,\sigma}. \tag{8}$$

By introducing Equation (8) in Equation (6) and thus eliminating v, we have

$$K_{w/s} = K_{w/o}^{zz} \cdot \left(1 - \frac{\theta}{\sigma} \cdot \frac{\mathrm{d}\,\sigma}{\mathrm{d}\,\theta} \cdot \frac{D_{s/o}^{zz}}{D_{w/o}^{zz}}\right). \tag{9}$$

According to Equation (9), we can calculate the hydraulic conductivity $K_{w/s}$ from the apparent conductivity $K_{w/o}^{zz}$, the measurements of water and solid contents θ and σ, the apparent diffusivities, and the shrinkage curve, which gives $\dfrac{\mathrm{d}\,\sigma}{\mathrm{d}\,\theta}$.

Suppose water evaporates from a cylindrical saturated clod by its open face and that its base is impervious. The water balance calculated for a clod layer extending from depth z_0 to the base of the clod for a Δt time increment is

$$\frac{\Delta V_w}{\Delta t} = - \oiint_{\Sigma = \Sigma_{bot} + \Sigma_{up} + \Sigma_{lat}} \mathbf{q}_{w/o} \cdot \mathbf{n} \cdot \mathrm{d}\Sigma, \tag{10}$$

where **n** is the unitary vector pointing outside the elementary surface $d\Sigma$. Σ is the outside surface of the clod layer. It is formed by the circular base Σ_{bot}, the upper circular surface Σ_{up} and the lateral surface Σ_{lat}. The water fluxes across Σ_{bot} and Σ_{lat} are nil and consequently are $\iint\limits_{\Sigma_{\text{bot}}+\Sigma_{\text{lat}}} \mathbf{q}_{\text{w/o}} \cdot \mathbf{n} \cdot d\Sigma$. The water balance becomes

$$\frac{\Delta V_{\text{w}}}{\Delta t} = q_{\text{w/o}}^{zz}(z_0,t) \cdot \Sigma_{\text{up}} = -D_{\text{w/o}}^{zz}\big(\theta(z_0,t)\big) \cdot \left(\frac{d\theta}{dz}\right)_{z_0,t} \cdot \Sigma_{\text{up}} \tag{11}$$

and we can then determine the apparent water diffusivity. A solid balance would give the same results for the solid apparent diffusivity. Having determined the diffusivities, we can calculate $K_{\text{w/s}}$ with Equation (9).

Laboratory measurements: experimental procedure

An undisturbed cylindrical soil core (45 cm in height and 8.5 cm in diameter) was sampled in the subsoil inside the prism delimited by cracks. The sampling was done after continued ponding followed by a little drying to allow cracks to open slightly in the prismatic layer. Two gravimetric water content profiles were determined, and small undisturbed aggregates were sampled in the immediate vicinity of the core. The water content, volume and structural porosity of these aggregates were measured and plotted on the shrinkage curve. Once in the laboratory, the 45-cm high core was cut into ten small cylindrical cores each 4.5 cm in height and 8.5 cm in diameter. Figure 1 shows that the evaporation rate decreases considerably when the open face was smoothed. In order to avoid this smoothing when preparing the small cores, hot air was applied at the upper surface of each small core for about 20 sec before starting the experiment. This created a mulch formed by millimetre-sized aggregates that closed the hydraulic path so water could not move vertically any more. The micro-aggregates were then chipped away with the tip of a flexible knife. By this way, the natural pores at the surface remained open, and the water content was still homogeneous inside the core.

Water was then allowed to evaporate from the upper surface of each core under

9

laboratory conditions (conditioned atmosphere at 24°C). The base of each core was sealed to prevent downward fluxes. As the core dried, it shrank, and shrinkage was greater at the top than at the bottom. The shape of the core became a frustrum of a cone, and this allowed evaporation from the sides. To prevent this evaporation the sides of the core were smoothed during sampling in the field and we put silicon grease between the core and cylindrical walls. By measuring the water content at different distances of the sample wall for two different clods, we made sure that the water content did not vary horizontally (see Figure 2). Each core was then studied at different time intervals. For a given core and a given time interval thirteen measurements of the total vertical shrinkage were first made with a vernier. The number of measurement locations was chosen to obtain a good accuracy of the mean height of the core (standard variation lower than 0.5 mm), the total time required for the measurement being less than 1 min. The diameter of the core was measured at the bottom, at 20 mm from the bottom and at the surface. The cross sectional areas could thus be calculated. The core was then cut into six thin layers of about 7 mm to measure gravimetric water content profiles. Volumetric water and solid contents and the matric potential could be deduced from the shrinkage and retention curves.

The water retention curve was determined by using the ultrafiltration apparatus of Tessier & Berrier (1979) for pressures less than 100 kPa, and the pressure plate apparatus for pressures between 100 kPa and 1600 kPa. Samples were initially saturated. The shrinkage curve was determined from small aggregates of a few cm^3. Some of the aggregates were sampled in the field at different moisture contents. They were thus subjected to the natural field overburden potential. Other aggregates came from those used for the water retention curve. The overburden potential was consequently removed from these aggregates. The volumes were obtained from buoyancy measurements in petroleum, the aggregates having been saturated in petroleum (Monnier *et al.*, 1973).

At specific instants, water and solid content profiles and matric potential profiles were

obtained. The apparent diffusivities were calculated according to Equation (11), and the apparent hydraulic conductivity $K_{w/o}^{zz}$ was obtained from the water balance and Equation (2). Equation (9) gave the Darcian hydraulic conductivity $K_{w/s}$.

Field measurements: theory

Material coordinates (subscript m) as described by Raats & Klute (1968, 1969) are used. The water balance on an elementary volume of a continuous ped without sinks and sources of water is

$$\left(\frac{\partial \vartheta}{\partial t}\right)_m = -\vec{\nabla}_m \cdot \mathbf{q}_{w/s} \, , \tag{12}$$

where $\vec{\nabla}_m$ is the vector differential operator expressed in the material coordinates of the solid phase and ϑ is the moisture ratio. Introducing Darcy's law into Equation (12), we get:

$$\left(\frac{\partial \vartheta}{\partial t}\right)_m = \vec{\nabla}_m \cdot \left(K_{w/s} \cdot \vec{\nabla}\phi\right), \tag{13}$$

where ϕ is the total potential of water and $\vec{\nabla}$ the vector differential operator expressed in a fixed coordinate system.

The deformation gradient tensor relating $\vec{\nabla}_m$ to $\vec{\nabla}$ is

$$\vec{\nabla}_m = \mathbf{J} \cdot \vec{\nabla}, \text{ with}$$

$$\mathbf{J} = \begin{bmatrix} \dfrac{\partial x}{\partial x_m} & \dfrac{\partial y}{\partial x_m} & \dfrac{\partial z}{\partial x_m} \\ \dfrac{\partial x}{\partial y_m} & \dfrac{\partial y}{\partial y_m} & \dfrac{\partial z}{\partial y_m} \\ \dfrac{\partial x}{\partial z_m} & \dfrac{\partial y}{\partial z_m} & \dfrac{\partial z}{\partial z_m} \end{bmatrix} \cdot \tag{14}$$

Combining Equation (14) with Equation (13) we obtain

$$\left(\frac{\partial \vartheta}{\partial t}\right)_m = \vec{\nabla}_m \cdot \left(\mathbf{K}_m \cdot \vec{\nabla}_m \phi\right) , \tag{15}$$

with

$$\mathbf{K}_m = K_{w/s} \cdot \mathbf{J}^{-1}. \tag{16}$$

Equation (15) is the same as Equation (20) of Raats & Klute (1968). When deformation and

11

flow occur in the vertical direction only, Raats & Klute (1969) wrote $\mathbf{J}$ as

$$\mathbf{J} = \begin{bmatrix} 1 & 0 & 0 \\ 0 & 1 & 0 \\ 0 & 0 & \dfrac{\rho_{d_0}}{\rho_d} \end{bmatrix}, \tag{17}$$

where ρ_d is the dry bulk density and ρ_{d_o} is the dry bulk density in an initial state. In general

cases, deformation occurs in every direction, and $\mathbf{J}$ is difficult to calculate (Raats & Klute,

1968; Vauclin, 1988). We propose calculating this matrix in the case of three-dimensional, but

not necessarily equidimensional, soil movements by formulating some hypotheses.

Hypothesis 1. Soil moves without shearing: in which case, the matrix $\mathbf{J}$ becomes diagonal and

can be written:

$$\mathbf{J} = \begin{bmatrix} \dfrac{d\,x}{d\,x_m} & 0 & 0 \\ 0 & \dfrac{d\,y}{d\,y_m} & 0 \\ 0 & 0 & \dfrac{d\,z}{d\,z_m} \end{bmatrix}. \tag{18}$$

For an elementary volume $\Delta V = \Delta x \cdot \Delta y \cdot \Delta z$, the corresponding material volume is

$$\Delta V_m = \frac{\Delta V}{1+e} = \Delta x_m \cdot \Delta y_m \cdot \Delta z_m, \tag{19}$$

where e is the void ratio. In the material coordinate system, the material volume is constant.

By differentiating equation (19) we have:

$$\frac{d(\Delta V_m)}{\Delta V_m} = 0 = \frac{d(\Delta x_m)}{\Delta x_m} + \frac{d(\Delta y_m)}{\Delta y_m} + \frac{d(\Delta z_m)}{\Delta z_m}. \tag{20}$$

Hypothesis 2. As for the one-dimensional flow and deformation where the material coordinate

is related to the fixed coordinate by the ratio $\dfrac{1}{1+e}$, we introduce β so that

12

$$\begin{cases} \Delta x_{\mathrm{m}} = \dfrac{\Delta x}{(1+e)^{\beta}} \\[2ex] \Delta y_{\mathrm{m}} = \dfrac{\Delta y}{(1+e)^{\beta}} \\[2ex] \Delta z_{\mathrm{m}} = \dfrac{\Delta z}{(1+e)^{1-2\cdot\beta}} \end{cases} \qquad . \tag{21}$$

Hypothesis 3. The soil deforms equidimensionally in the horizontal plane. Voltz & Cabidoche (1995) defined the anisotropic ratio k as the ratio between vertical and horizontal elongation rates:

$$k = \frac{\left(\mathrm{d}(\Delta x)\big/\Delta x\right)}{\left(\mathrm{d}(\Delta z)\big/\Delta z\right)} = \frac{\left(\mathrm{d}(\Delta y)\big/\Delta y\right)}{\left(\mathrm{d}(\Delta z)\big/\Delta z\right)}. \tag{22}$$

Hypothesis 4. We look for β so that

$$\frac{\mathrm{d}(\Delta x_{\mathrm{m}})}{\Delta x_{\mathrm{m}}} = \frac{\mathrm{d}(\Delta y_{\mathrm{m}})}{\Delta y_{\mathrm{m}}} = \frac{\mathrm{d}(\Delta z_{\mathrm{m}})}{\Delta z_{\mathrm{m}}} = 0. \tag{23}$$

Equation (23) is different from Equation (20), which comes from the mass conservation of solid particles. Now, from Equation (21) we have

$$\mathrm{d}(\Delta x_{\mathrm{m}}) = \frac{\mathrm{d}(\Delta x)}{(1+e)^{\beta}} - \beta \cdot \frac{\Delta x}{(1+e)^{\beta}} \cdot \frac{\mathrm{d}e}{1+e} \quad . \tag{24}$$

By definition, we have

$$\frac{\mathrm{d}e}{1+e} = \frac{\mathrm{d}(1+e)}{1+e} = \frac{\mathrm{d}(\Delta V)}{\Delta V} = \frac{\mathrm{d}(\Delta x)}{\Delta x} + \frac{\mathrm{d}(\Delta y)}{\Delta y} + \frac{\mathrm{d}(\Delta z)}{\Delta z} \quad . \tag{25}$$

Equation (25) becomes by using Equation (22):

$$\frac{\mathrm{d}e}{1+e} = (1+2\cdot k) \cdot \frac{\mathrm{d}(\Delta z)}{\Delta z} = \frac{(1+2\cdot k)}{k} \cdot \frac{\mathrm{d}(\Delta x)}{\Delta x} = \frac{(1+2\cdot k)}{k} \cdot \frac{\mathrm{d}(\Delta y)}{\Delta y}. \tag{26}$$

Thus, when we put Equation (26) into Equation (24) and then Equation (24) into Equation (23), the fourth hypothesis becomes

$$\beta = \frac{k}{1+2\cdot k} \quad , \tag{27}$$

and putting Equation (27) into Equation (16) the material hydraulic conductivity tensor $\mathbf{K}_m$ can be written

$$\mathbf{K}_m = \begin{bmatrix} K_m^h & 0 & 0 \\ 0 & K_m^h & 0 \\ 0 & 0 & K_m^v \end{bmatrix} = \begin{bmatrix} \dfrac{K_{w/s}}{(1+e)^\beta} & 0 & 0 \\ 0 & \dfrac{K_{w/s}}{(1+e)^\beta} & 0 \\ 0 & 0 & \dfrac{K_{w/s}}{(1+e)^{1-2\cdot\beta}} \end{bmatrix}. \tag{28}$$

Equation (15) and the above-mentioned material conductivity tensor are equivalent to the results of Garnier (1996). This tensor can be written as a scalar if $K_m^h = K_m^v$, which is equivalent to

$$\beta = 1 - 2\cdot\beta \Leftrightarrow \beta = \frac{1}{3} \Leftrightarrow k = 1, \tag{29}$$

i.e. when soil deformation is isotropic. For the vertisol studied, Cabidoche & Ozier-Lafontaine (1995) found an anisotropic ratio of 0.85: vertical movements were more important than horizontal ones. With this value, Equation (27) implies $\beta < \frac{1}{3}$, and thus $K_m^h < K_m^v$.

In the case of vertical one-dimensional soil movement and water flow, the ratio k is nil -see equation (22)- as is α according to Equation (27). Equation (15) becomes

$$\left(\frac{\partial \vartheta}{\partial t}\right)_m = \frac{\partial}{\partial z_m}\left(K_m \cdot \frac{\partial\left(\psi_m - z + \Omega\right)}{\partial z_m}\right), \tag{30}$$

with

$$K_m = \frac{K_{w/s}}{1+e} . \tag{31}$$

Equations (30) and (31) are equivalent to the relation (9) of Philip (1969), relations (12) and (13a) of Angulo *et al.* (1990a), (14) of Kim *et al.* (1992a). Hence, our theory reduces to the existing theory for one-dimensional fluxes.

If the matric potential is uniform in a horizontal plane then the water flows only vertically but soil deforms three-dimensional still. In that case we get Equation (30) from

Equation (15), but Equation (31) is now

$$K_{\mathrm{m}} = \frac{K_{\mathrm{w/s}}}{\left(1+e\right)^{1-2\cdot\beta}} \quad.$$
(32)

Field measurements: experimental procedures

We used a transducer named THERESA that measured thickness changes of soil layers. It was designed by taking into account the intrinsic properties of vertisols. Its conditions of use were described in Cabidoche & Voltz (1995) and in Cabidoche & Ozier-Lafontaine (1995). The model relating thicknesses and the gravimetric water content is described in Voltz & Cabidoche (1995). We supposed a constriction of the structural porosity along the normal phase of shrinkage proportional to matric shrinkage (McGarry & Daniells, 1987; Cabidoche & Voltz, 1995). Thirty transducers were set up in the experimental parcel during three periods between 1993 and 1996. Five soil layers were investigated with six replicates for each depth. This led to a good accuracy of $0.02 \ \mathrm{kg \ kg^{-1}}$ for the calculation of the mean water content (Cabidoche & Ozier-Lafontaine, 1995). We supposed that the average water content profile changes were caused by vertical matric flow only. No exchange was supposed to occur from either structural to matric porosity or from cracks to matric porosity. The experimental parcel was drained by a network of pipes 16 m apart and 1.1 m deep. Hydrographs were installed at triangular weirs to record overland flow and drainage. We studied rewetting of the profile during and after each rainfall event not followed neither by drainage nor by runoff. At the bottom of the profile (1.20 m in depth) an impervious layer prevented downward water fluxes. A water balance was made from the impervious base to the depth of 80 cm and 50 cm. By using the instantaneous profile method, the vertical material hydraulic conductivity could be calculated from Equations (30) and (32), assuming vertical water flow and three-dimensional deformation of the soil.

Results and discussion

The shrinkage curve is plotted in Figure 3a (*W* against *v*) and in Figure 3b (θ against σ). No difference can be observed between the aggregates sampled in the field and subjected to the overburden and the other aggregates in which the overburden was removed. This result and the uniform value of 0.85 of the ratio *k* with depth (Cabidoche & Voltz, 1995) show that the overburden potential does not influence soil properties. It contrasts with the results of Bronswijk (1990) who investigated unripe wet marine clay soil.

The retention curve is plotted in Figure 4 and fitted with the model of Van Genuchten (1980). In the laboratory studies, three sets of cores were sampled. We plotted on the shrinkage curve the initial conditions of each set at the beginning of the experiment (Figure 3a). The initial conditions of each set were measured on the small aggregates sampled near the core (see *Laboratory measurements: experimental procedure*, first paragraph). This shows that structural porosity does not contain water and that water fluxes are only matric fluxes. The instantaneous profiles for these sets are plotted in Figure 5a,b and c for the water content, and in Figure 6a,b and c for the solid content. The ratio between the apparent conductivity $K_{w/o}^{zz}$ and $K_{w/s}$ is plotted in Figure 7. This ratio ranges from 1 for dry soil to 5 when wet, the discrepancy being larger for the wetter soil. Nakano *et al.* (1986) and Angulo *et al.* (1990b) found a ratio ranging from 1 to 3 for bentonite pastes.

In the field the model of Voltz & Cabidoche (1995) was used to calculate the gravimetric water content and specific volume of peds, and thus the volumetric water content. In Figure 8 we plotted the $K_{w/s}$ obtained in laboratory experiments and in the field.

The Darcian conductivity results show little variation when the soil is dry, but they are more variable for wet soil. The polynomial adjustment of degree 3 gives a conductivity value of 0.2 cm day^{-1} for a water content of 0.570 m^{-3} m^{-3} (matric potential of -3 kPa). Ritchie *et al.* (1972a) found an apparent conductivity of 0.03 cm day^{-1} at the same matric potential in vertisols from Texas and a field saturated conductivity of 0.1 cm day^{-1} (Ritchie *et al.*, 1972b). Douglas & McKyes (1978) measured a material conductivity of 0.08 cm day^{-1} for a matric

potential of -0.1 kPa in a remodelled clay soil. The field measurements are more variable, but our experimental plot can be partly responsible for it. During the three measurement periods during several months, we could retain the rain on only three occasions to satisfy our assumptions about vertical water flow. Moreover, these events were quickly followed (several hours later) either by more heavy rain that caused drainage or runoff, or by water absorption by plant roots. The changes in thickness and water contents were then small. Indeed, the water content changes were of the same order of magnitude as the experimental accuracy. Nevertheless despite this variation, the conductivities calculated from the field experiment are always one order of magnitude greater than the conductivities obtained in the laboratory. Some authors (Flühler *et al.*, 1976) found significant differences between the *in situ* hydraulic conductivity and the conductivity determined in the laboratory, especially for fine textured swelling soils. In our case, as *in situ* and laboratory measurements were conducted under wetting and drying conditions respectively, we can consider that a physical hysteresis is responsible for this discrepancy. We discuss this hypothesis below.

This hysteresis cannot be caused by bypass flow in the structural porosity because exchange of water from structural porosity to matric porosity is almost nil. Moreover, the transducers make it possible to measure the matric water content only. Preferential flow paths along slickensides must also be rejected because, in the soil we studied, the slickensides are just failure planes and have negligible volume. It seems questionable to explain this hysteresis by a bypass flow in the biggest matric pores: on the one hand, these pores are saturated as far as the flow occurs in the normal phase of the shrinkage curve, and on the other, the size of these pores is less than 2 μm. The larger value of conductivity measured during wetting could be caused by micro-cracks along the wetting front. Stengel (1983) observed this phenomenon in the field at the surface of the soil. In our experiments, as cracks remained open in the deep layers, the volume of these cracks enabled micro-cracks to appear when the peds rewetted. Last our hypothesis concerning vertical water flow could be wrong. Owing to the spatial

variation of the network of cracks and soil characteristics, water can enter cracks in a part of the field plot even if no drainage is recorded. This water can then wet the peds horizontally. Consequently some of the transducers near the axes of the prisms measured variations in thickness due to vertical flow only and elsewhere those near crack walls measured changes caused by both vertical and horizontal flow.

For the three periods that we studied, we plotted the 90 % confidence interval of the estimation of the mean water content (Figure 8). Taking into account this spatial variation, we can see that the field conductivities are in the same range as those recorded at the laboratory. Thus, we cannot conclude that physical hysteresis is responsible for the discrepancy between field and laboratory measurements.

We made calculations by both incorporating and not incorporating the overburden potential in the total potential for the field experiment. The conductivities calculated with the overburden potential were found to be not significantly different (at a 5 % level) from the conductivities calculated without taking into account the overburden potential. This is because the gradients of overburden potential (about 1 m m^{-1}) are smaller than those of matric potentials (about 70 m m^{-1}).

Conclusions

We have presented a laboratory method to measure the apparent and Darcian hydraulic conductivity of the matric porosity of a vertisol as a function of the water content under drying conditions. The theory deals with solid deformation and water flow in every direction and describes water flow in a Eulerian coordinate system. In our experiments, we restricted to vertical water flow only and we ensured that water flowed only in the matric porosity. Millimetre-sized aggregates were removed from the side of the core so that the natural pores at the surface remained open and water could evaporate from them. Thus smoothing effects on the evaporation rate were avoided. Under rewetting conditions, the Darcian conductivity was

measured in the field using a material coordinate system. The equations developed for that take into account vertical and horizontal soil movements and water flow. The deformations were not assumed to be equidimensional. Nevertheless, even if we suppose in our theory that soil movements are free of shear, which is probably not true, nothing more satisfactory can be used to describe three-dimensional water fluxes and soil movement.

We showed that the overburden potential did not influence soil properties and that its gradient was smaller than the gradient of the matric potential. The ratio between field conductivity and laboratory conductivity was about 10. This discrepancy may be explained by a hysteresis caused by a network of fine cracks that develops during the rewetting of the peds, but our results did not allow us to draw a final conclusion.

References

Angulo, R., Gaudet, J. P., Thony, J. L. & Vauclin, M. 1990a. Conductivité hydraulique d'un milieu poreux partiellement saturé, déformable. I. Principes de détermination. *Comptes Rendus de l'Académie des Sciences de Paris*, *série II*, **310**, 161 - 164.

Angulo, R., Gaudet, J. P., Thony, J. L. & Vauclin, M. 1990b. Conductivité hydraulique d'un milieu poreux partiellement saturé, déformable. II. Résultats expérimentaux. *Comptes Rendus de l'Académie des Sciences de Paris*, *série II*, **310**, 341 - 345.

Bronswijk, J.J.B. 1990. Shrinkage geometry of a heavy clay soil at various stresses. *Soil Science Society of America Journal*, **54**, 1500 - 1502.

Cabidoche, Y.-M. & Ozier-Lafontaine, H. 1995. THERESA: I. Matric water content measurements through thickness variations in vertisols. *Agricultural Water Management*, **28**, 133 - 147.

Cabidoche, Y.-M. & Voltz, M. 1995. Non-uniform volume and water content changes in swelling clay soil: II. A field study on a Vertisol. *European Journal of Soil Science*, **46**, 345 - 355.

Douglas, E. & McKyes, E. 1978. Compaction effects on the hydraulic conductivity of a clay soil. *Soil Science*, **125**, 278 - 282.

Douglas, E., McKyes, E., Taylor, F., Negi, S. & Raghavan, G. S. V. 1980. Unsaturated hydraulic conductivity of a tilled clay soil. *Canadian Agricultural Engineering*, **22**, 153 - 161.

Flühler, H., Germann, P., Richard, F. & Leuenberger, J. 1976. Bestimmung von hydraulischen Parametern für die Wasserhaushaltsuntersuchungen im natürlichen gelagerten Boden. Ein Vergleich von Feld- und Laboratoriumsmethoden. *Zeitschrift für Pflanzenernährung und Bodenkunde*, **139**, 329 - 342.

Garnier, P. 1996. *Détermination des caractéristiques hydrodynamiques de sols déformables par la méthode inverse*. Thèse de doctorat de l'Université de Nancy I, Nancy.

Jarvis, N. J., Leeds-Harrison, P. B. & Dosser, J.M. 1987. The use of tension infiltrometers to assess routes and rates of infiltration in a clay soil. *Journal of Soil Science*, **38** , 633-640.

Jarvis, N. J. & Messing, I. 1995. Near-saturated hydraulic conductivity in soils of contrasting texture measured by tension infiltrometers. *Soil Science Society of America Journal*, **59**, 27 - 34.

Kim, D. J., Diels, J. & Feyen, J. 1992a. Water movement associated with overburden potential in a shrinking marine clay soil. *Journal of Hydrology*, **133**, 179 - 200.

Kim, D. J., Vereecken, H., Feyen, J., Boels, D. & Bronswijk, J. J. B. 1992b. On the characterization of properties of an unripe marine clay soil II. A method on the determination of hydraulic properties. *Soil Science*, **154**, 59 - 71.

McGarry, D. & Daniells, I.G. 1987. Shrinkage curve indices to quantify cultivation effects on soil structure of a Vertisol. *Soil Science Society of America Journal*, **51**, 1575 - 1580.

McIntyre, D.S. & Sleeman, J. R. 1982. Macropores and hydraulic conductivity in a swelling soil. *Australian Journal of Soil Research*, **20**, 251 - 254.

Monnier, G., Stengel, P. & Fiès, J.C. 1973. Une méthode de mesure de la densité apparente de petits agglomérats terreux. Application à l'analyse des systèmes de porosité du sol. *Annales Agronomiques*, **24**, 533 - 545.

Nakano, M., Amemiya, Y. & Fujii, K. 1986. Saturated and unsaturated hydraulic conductivity of swelling clays. *Soil Science*, **141**, 1 - 6.

Philip, J.R. 1969. Hydrostatics and hydrodynamics in swelling soils. *Water Resources Research*, **5**, 1070 - 1077.

Raats, P.A.C. & Klute, A. 1968. Transport in soils: the balance of mass. *Soil Science Society of America Proceedings*, **32**, 161 - 166.

Raats, P.A.C. & Klute, A. 1969. One-dimensional, simultaneous motion of the aqueous phase and the solid phase of saturated and partially saturated porous media. *Soil Science*, **107**, 329 - 333.

Ritchie, J. T., Burnett, E. & Henderson, R.C. 1972a. Dryland evaporation flux in a subhumid climate: III. Soil water influence. *Agronomy Journal*, **64**, 168 - 173.

Ritchie, J. T., Kissel, D. E. & Burnett, E. 1972b. Water movement in undisturbed swelling clay soil. *Soil Science Society of America Proceedings*, **36**, 874 - 879.

Smiles, D.E. & Harvey, A.G. 1973. Measurement of moisture diffusivity of wet swelling systems. *Soil Science*, **116**, 391 - 399.

Stengel, P. 1983. Cracks formation during swelling: effects on soil structure regeneration after compaction. In: *Proceedings Tillage and Traffic in Crop Production, volume 1* (ed. ISTRO, Haren), pp. 147 - 152. International Soil Tillage Research Organization, Haren.

Stirk, G.B. 1954. Some aspects of soil shrinkage and the effect of cracking upon water entry into the soil. *Australian Journal of Agricultural Research*, **5**, 279-290.

Tessier, D. & Berrier, J. 1979. Utilisation de la microscopie électronique à balayage dans l'étude des sols. *Science du Sol*, **1**, 67 - 82.

Van Genuchten, M.T. 1980. A closed-form equation for predicting the hydraulic conductivity of unsaturated soils. *Soil Science Society of America Journal*, **44**, 892 - 898.

Vauclin, M. 1988. Hydrodynamique des sols partiellement saturés déformables. In: *Les phénomènes de transfert dans les milieux poreux déformables* (ed. INRA-Département de Science du Sol, Versailles), pp. 62 - 113. INRA Edition, Paris.

Voltz, M. & Cabidoche, Y.-M. 1995. Non-uniform volume and water content changes in swelling clay soil: I. Theoretical analysis. *European Journal of Soil Science*, **46**, 333 - 343.

List of Figures

Fig. 8 Darcian unsaturated hydraulic conductivity of the matric porosity measured in the field and in the laboratory. The polynomial regression was performed upon laboratory results. Horizontal bars represent the 90 % confidence interval of the estimation of the mean water content due to spatial variation in the field experiment.
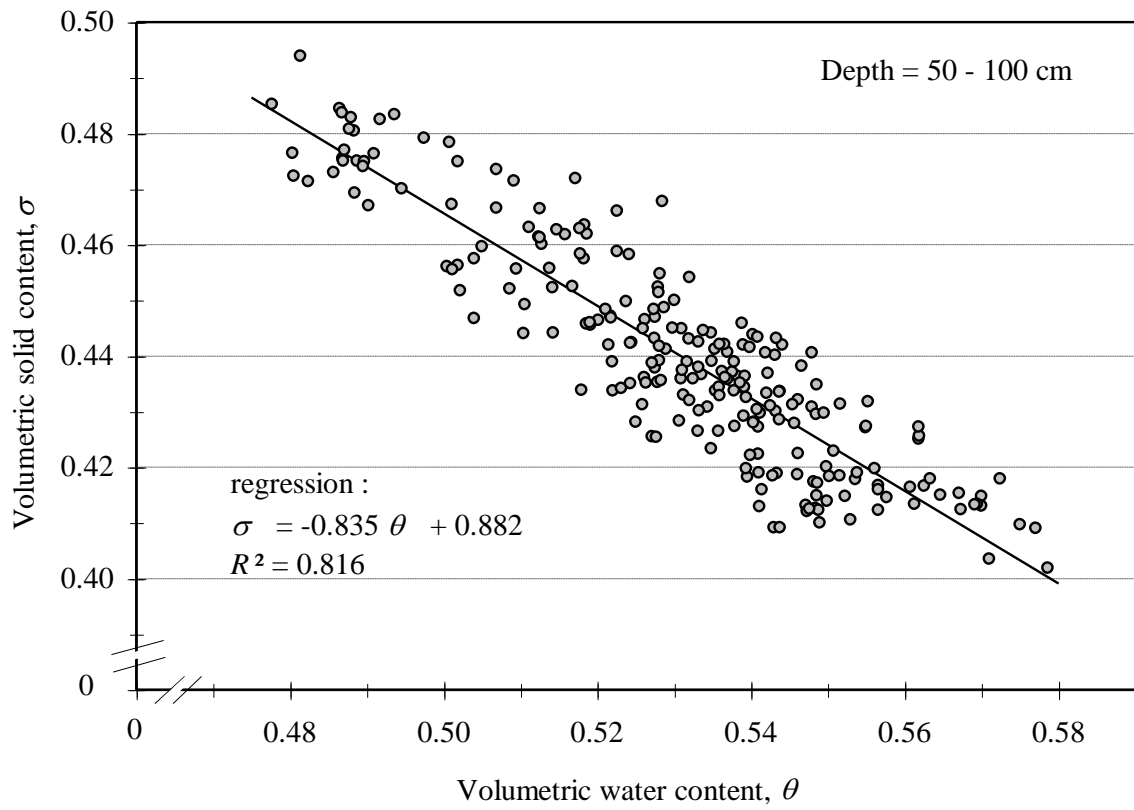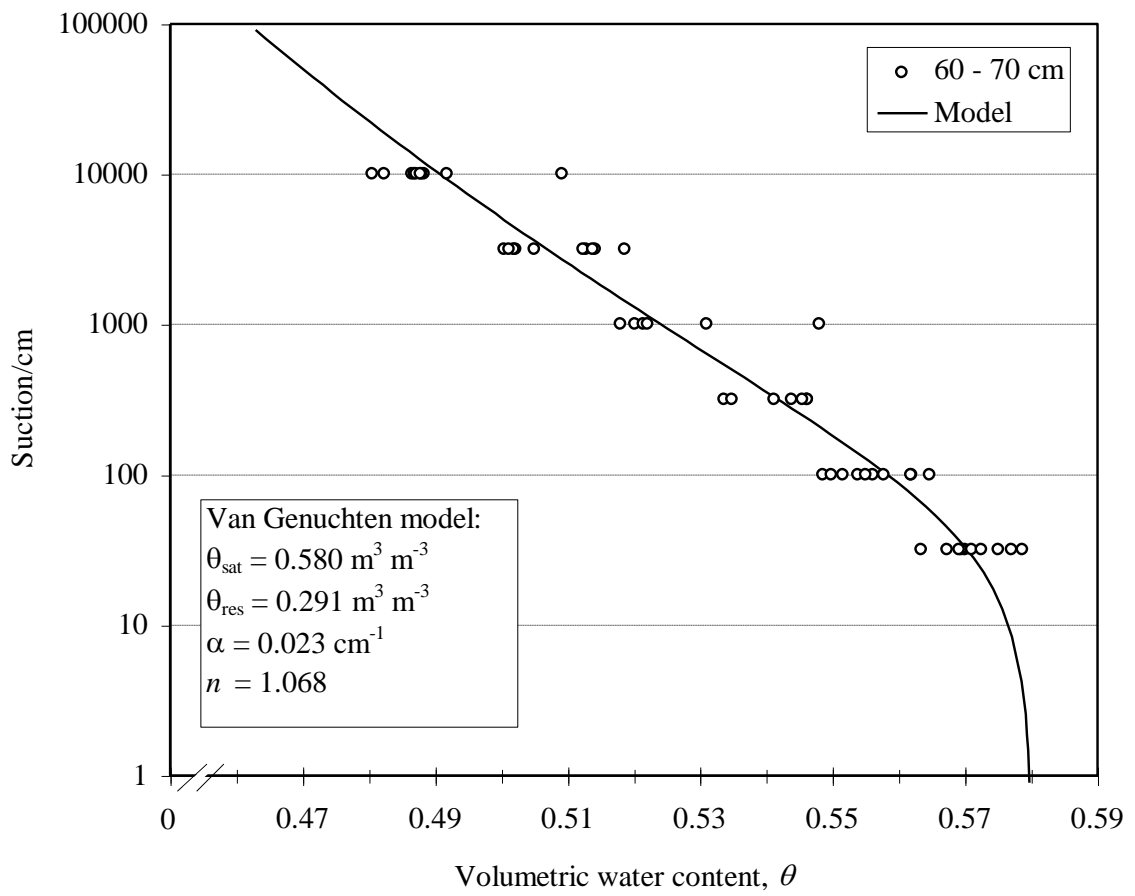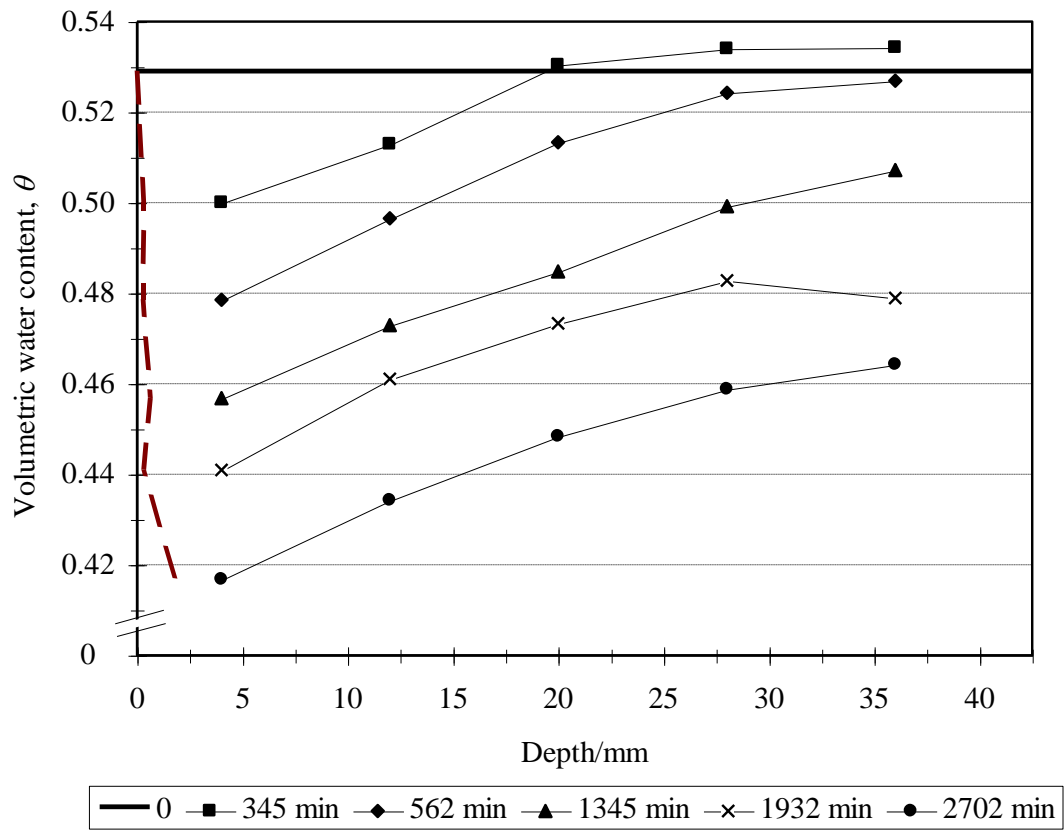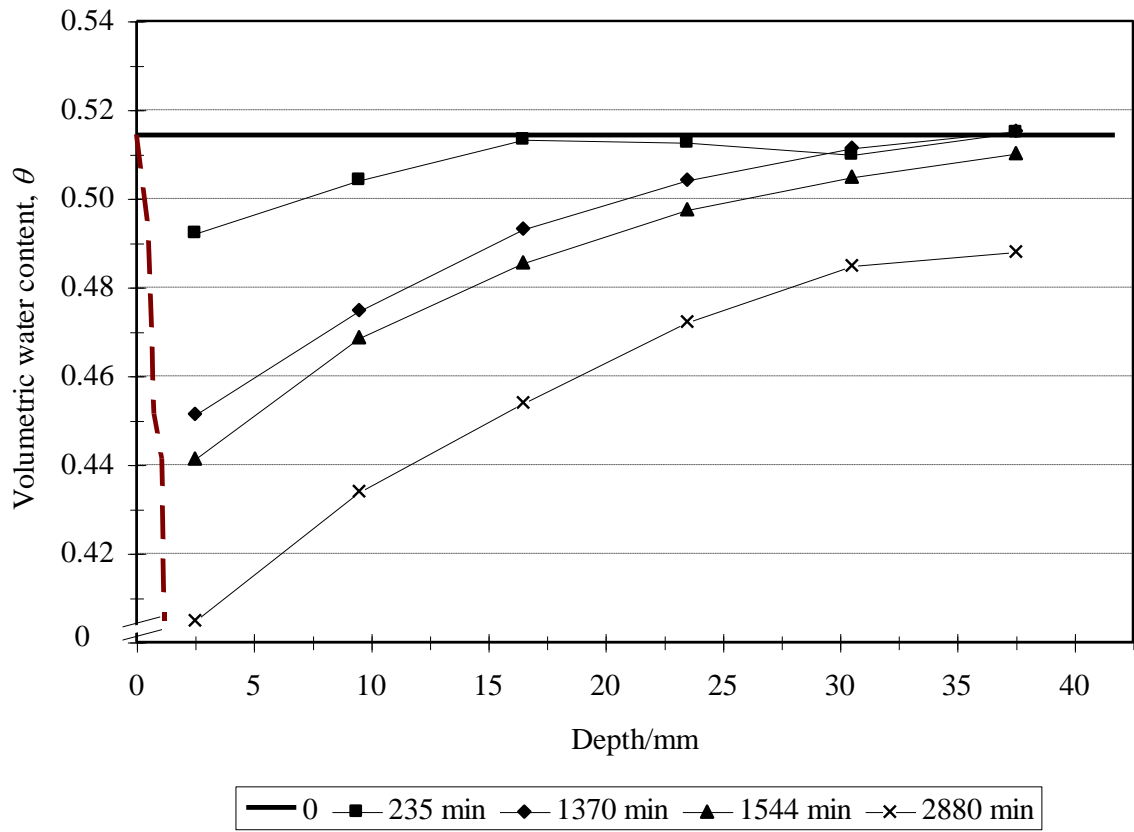
Figure 1
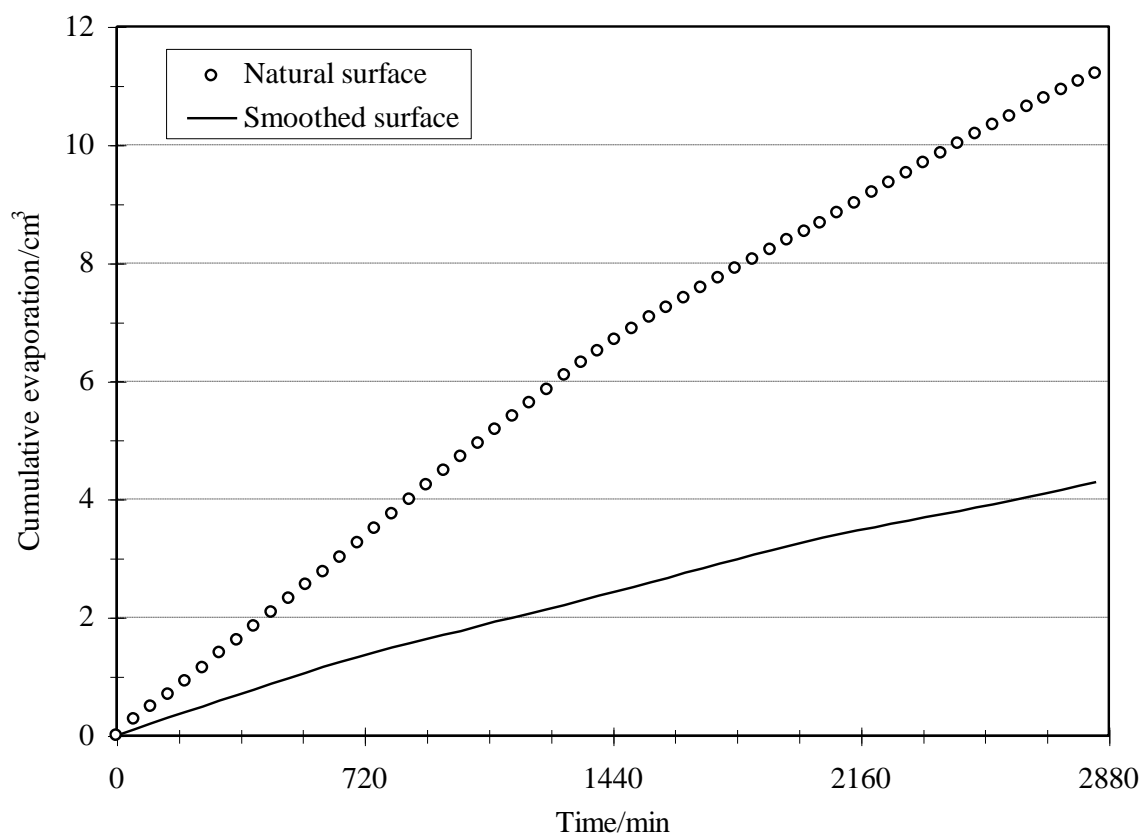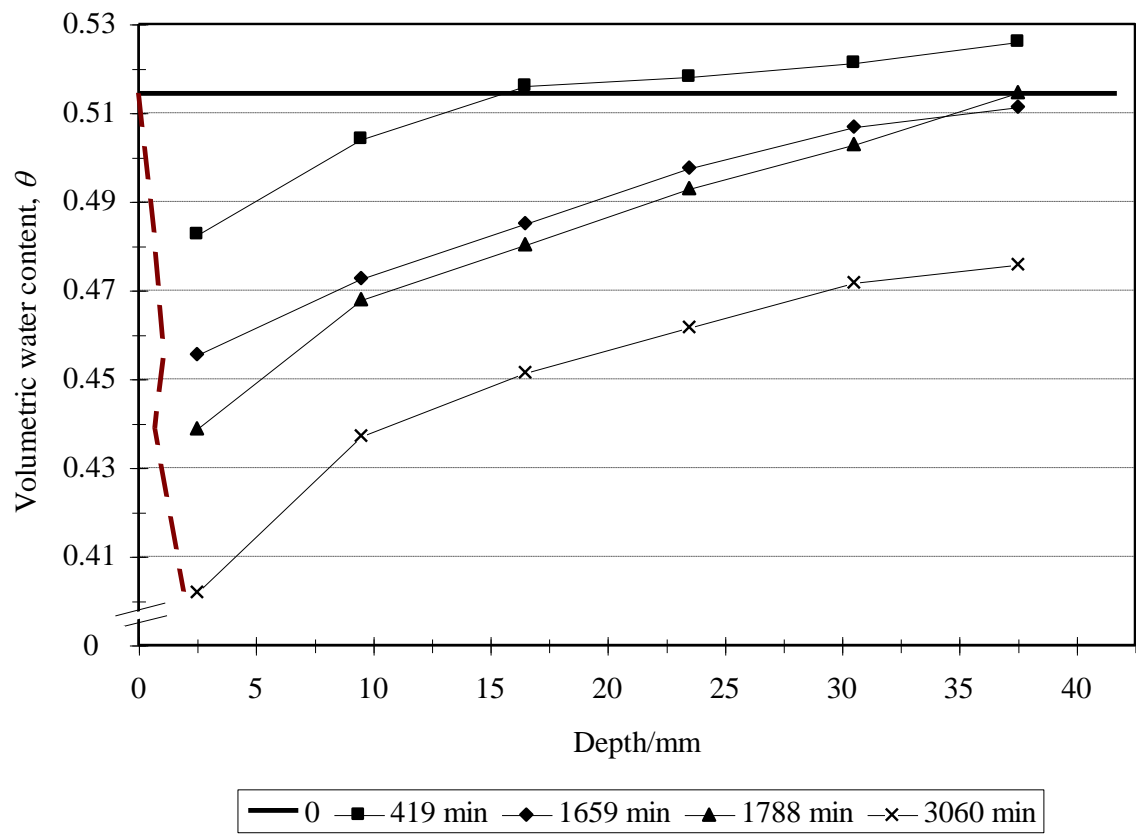
Figure 2a:
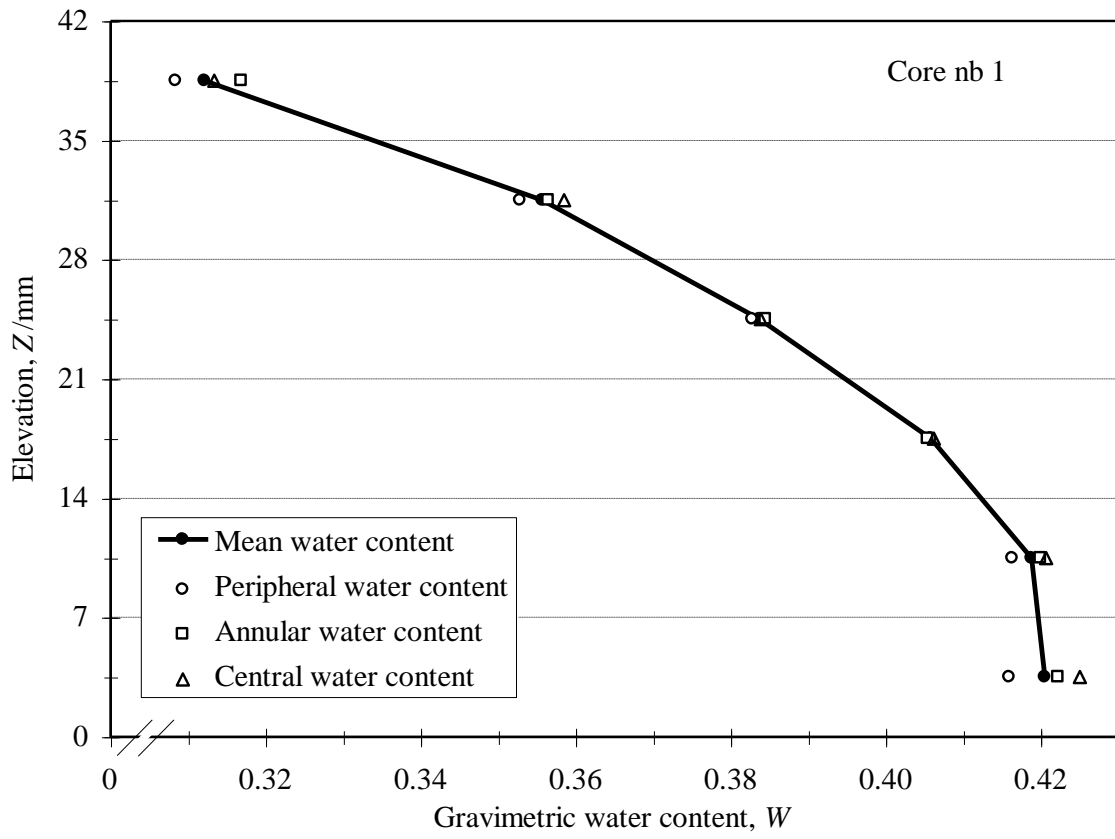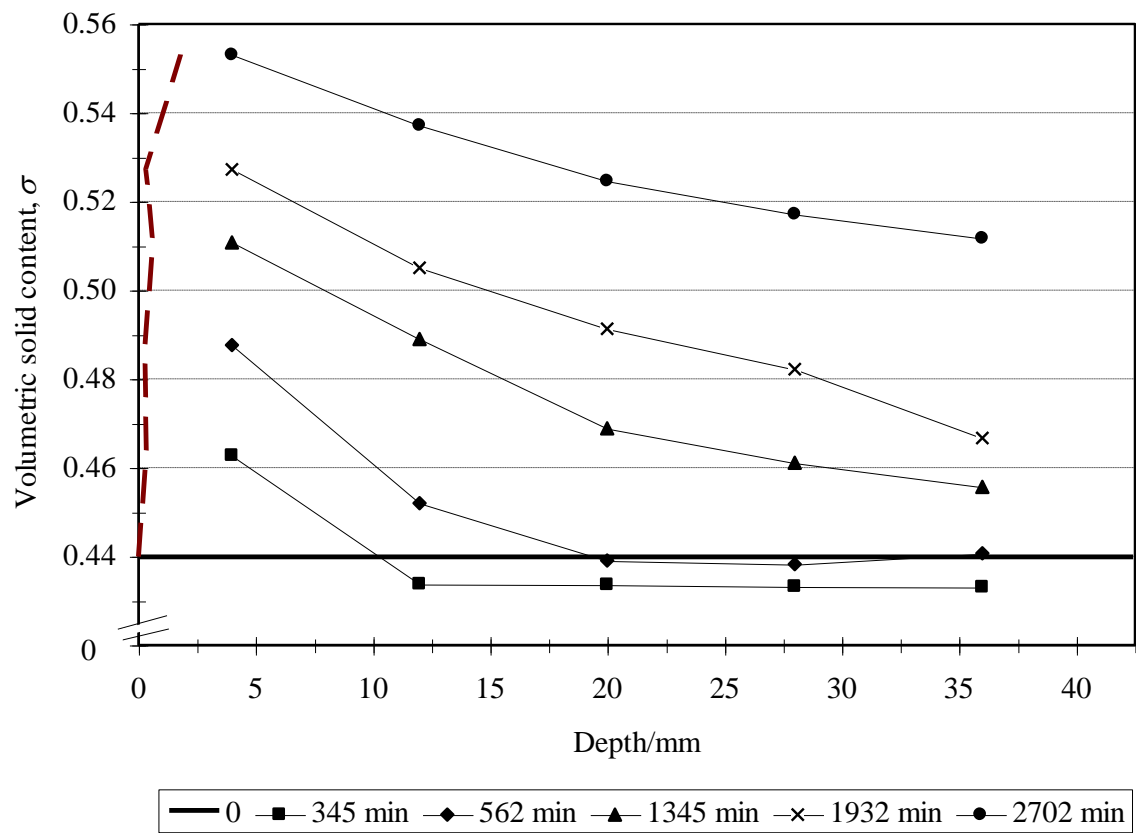
Figure 2b:
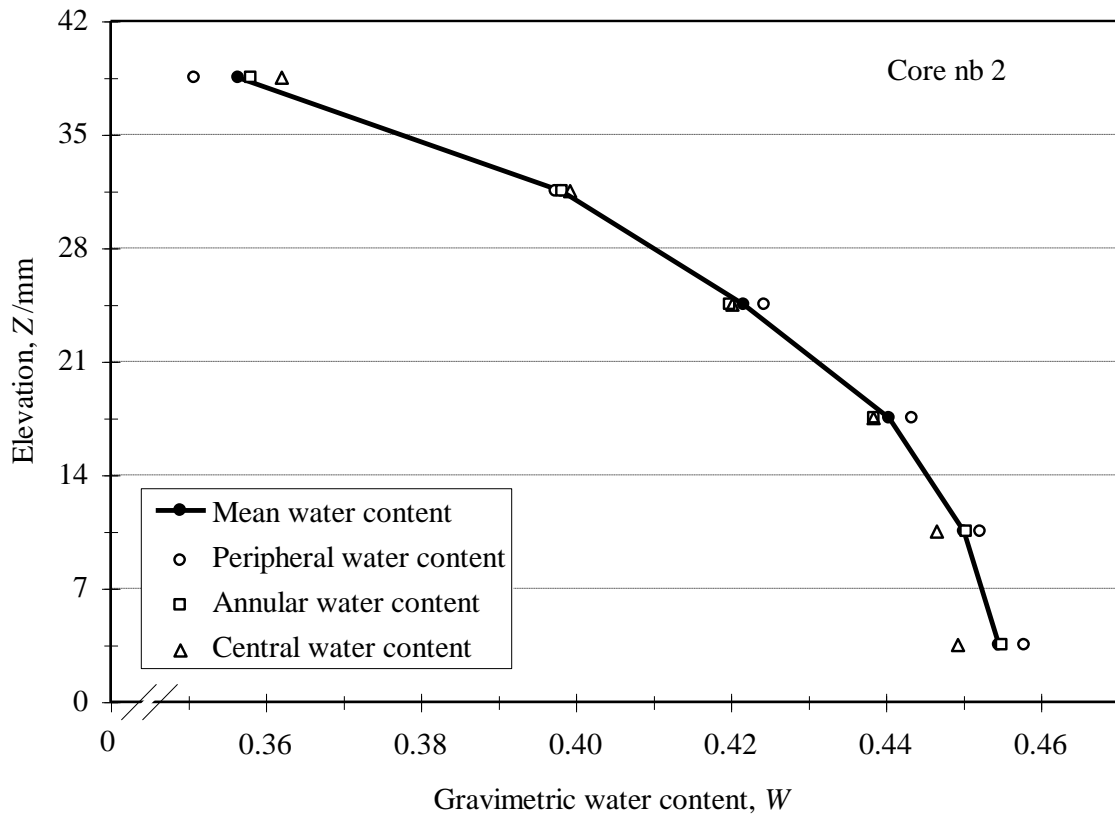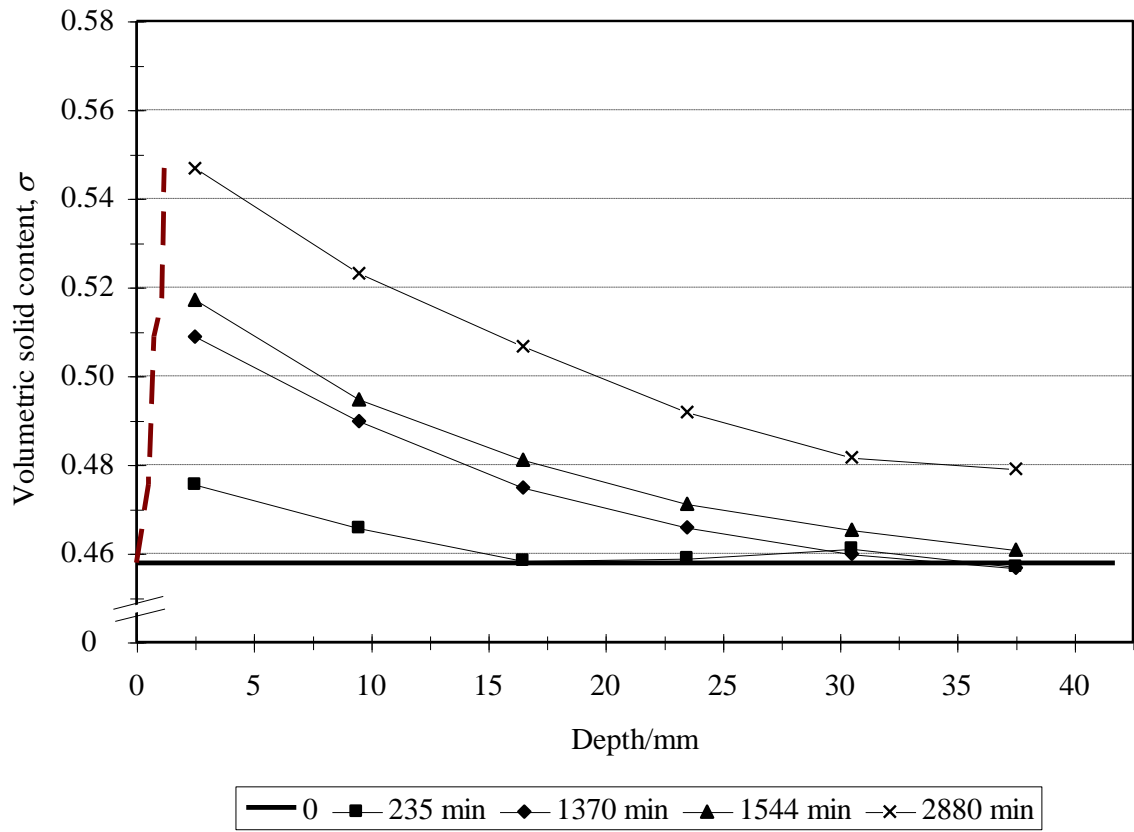
Figure 3a:
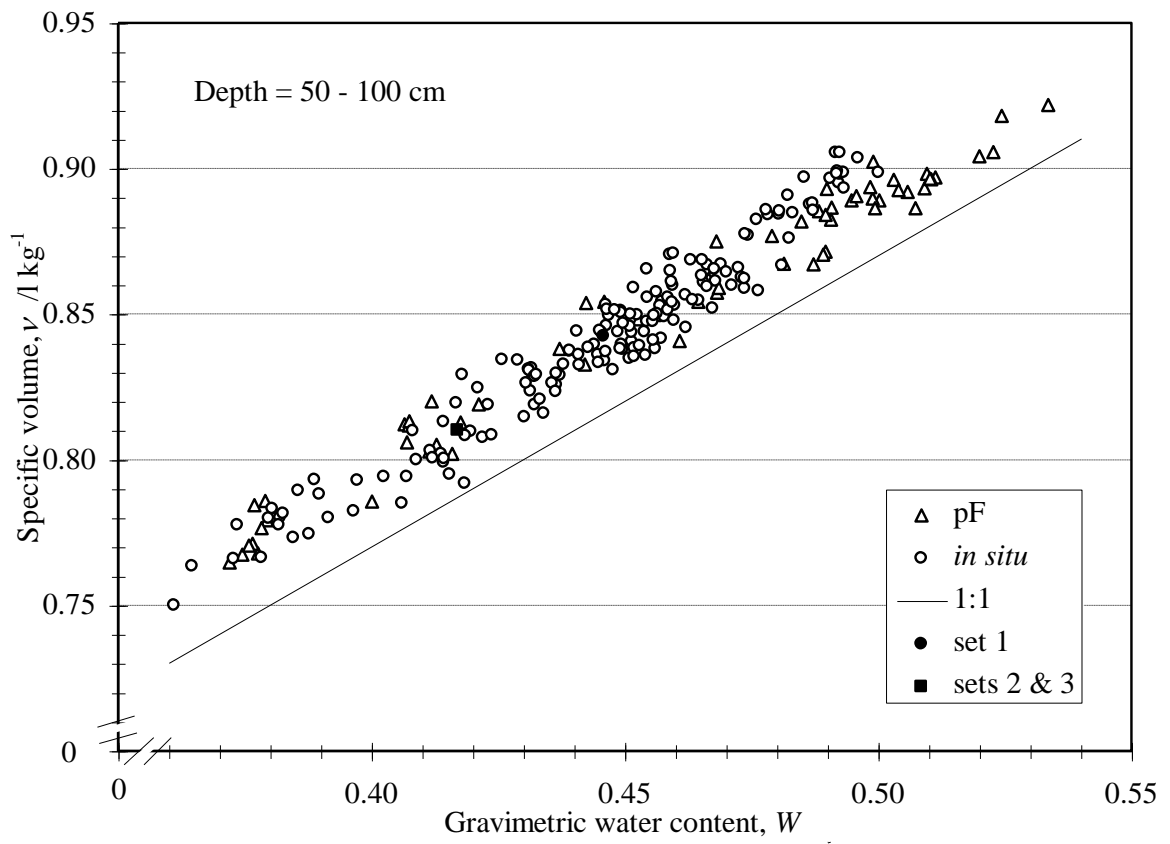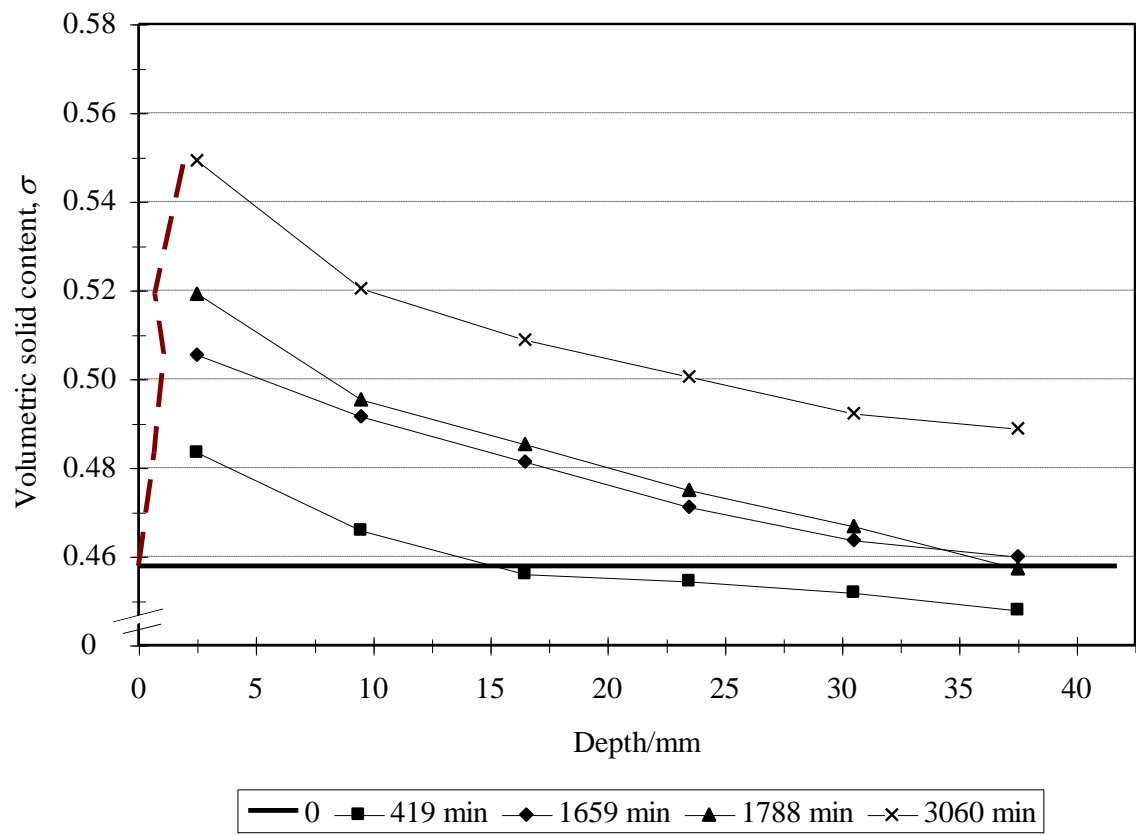
Figure 3b:
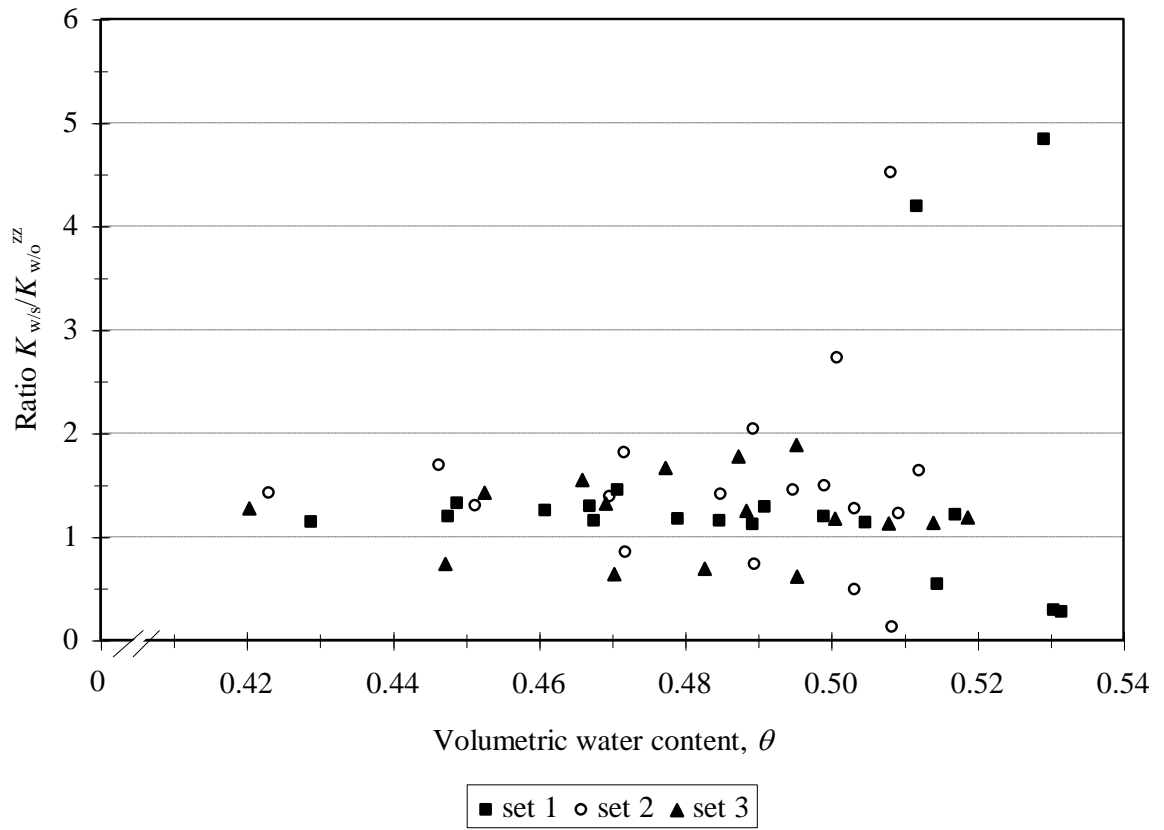
Figure 4:

Figure 5a:

Figure 5b:

Figure 5c:

Figure 6a:

Figure 6b:

Figure 6c:

Figure 7:

Figure 8: